

Journal of Innovative Clinical Trials and Case Reports

ISSN: 3068 - 1936

DOI: doi.org/10.63721/25JCTC0104

Analysis and Control of Brain Dynamic Models

Lakshmi N Sridhar

Chemical Engineering Department, University of Puerto Rico, Mayaguez, PR 00681, USA

Citation: Lakshmi N Sridhar (2025) Analysis and Control of Brain Dynamic Models. J of Inn Clin Trail Case Reports 1(1): 01-10. WMJ/JICTCR-104

Abstract

The nonlinear behavior of the brain's information processing represents one of the key tasks in modern neuroscience, and a lot of research has been conducted in trying to rhythmicity in brain networks. Bifurcation analysis is a powerful mathematical tool used to deal with the nonlinear dynamics of any process. Several factors must be considered, and multiple objectives must be met simultaneously. Bifurcation analysis and multiobjective nonlinear model predictive control (MNLMPC) calculations are performed on two brain dynamic models. The MATLAB program MATCONT was used to perform the bifurcation analysis. The MNLMPC calculations were performed using the optimization language PYOMO in conjunction with the state-of-the-art global optimization solvers IPOPT and BARON. The bifurcation analysis Hopf bifurcation points that lead to limit cycles in the two models. These Hopf points were eliminated using an activation factor that involves the tanh function. The multiobjective nonlinear model predictive control calculations converge to the Utopia point in both the problems, which is the best solution.

*Corresponding author: Lakshmi N Sridhar, Chemical Engineering Department, University of Puerto Rico, Mayaguez, PR 00681, USA.

Submitted: 14.05.2025 **Accepted:** 21.05.2025 **Published:** 26.05.2025

Keywords: Bifurcation, Optimization, Control, Neuroscience, Brain Hopf

Background

Yamaguchi showed that lecticans are organizers of the brain's extracellular matrix [1]. Manor et al. showed that synaptic depression mediates bistability in neuronal networks with recurrent inhibitory connectivity [2]. Oohashi et al demonstrated that Brall, a brain-specific link protein, colocalizes with the

versican v2 isoform at the nodes of Ranvier in developing and adult mouse central nervous systems [3]. Bekku et al performed the molecular cloning of bral2, a novel brain-specific link protein, and demonstrated the immunohistochemical colocalization with brevican in perineuronal nets [4]. Dityatev et al showed the synaptic plasticity of extracellular matrix molecules [5].

Carulli et al. determined the composition of perineuronal nets in the adult rat cerebellum and the cellular origin of their components [6].

Rich and Wenner researched sensing and expressing homeostatic synaptic plasticity [7]. Dityatev et al. investigated the activity-dependent formation and functions of chondroitin sulfate-rich extracellular matrix of perineuronal nets [8]. Turrigiano showed that homeostatic signaling was the positive side of negative feedback [9]. Xie et al. demonstrated the existence of Hopf bifurcations in the Hodgkin-Huxley model [10]. Cingolani et al. the activity-dependent regulation of synaptic AMPA receptor composition and abundance by beta 3 integrins [11].

Durstewitz discussed the implications of synaptic biophysics for recurrent network dynamics and active memory [12]. Dityatev remodeled the extracellular matrix and epileptogenesis [13]. Kochlamazashvili et al. that the extracellular matrix molecule hyaluronic acid regulates hippocampal synaptic plasticity by modulating postsynaptic 1-type ca(2+) channels [14]. Dityatev et al. demonstrated that the extracellular matrix played a dual role in synaptic plasticity and homeostasis [15]. Dityatev and Rusakov demonstrated the existence of molecular signals of plasticity at the tetrapartite synapse [16]. Włodarczyk et al. showed the role played by extracellular matrix molecules, their receptors, and secreted proteases in synaptic plasticity [17]. Kazantsev et al. developed a homeostatic model of neuronal firing governed by feedback signals from the extracellular matrix [18].

Soleman et al. investigated the targeting of the neural extracellular matrix in neurological disorders [19]. Dembitskaya et al. Studied the effects of enzymatic removal of chondroitin sulfates on neural excitability and synaptic plasticity in the hippocampal CA1 region [20]. Favuzzi et al. investigated the activity-dependent gating of parvalbumin interneuron function by the perineuronal net protein brevican [21]. Jercog et al demonstrated that the cortical dynamics reflect state transitions in a bistable network [22]. Schmidt et al. showed that the network mechanisms cause oscillations in cognitive tasks [23]. Azeez et al. demonstrated the diurnal fluctuation of extracellular matrix organization in the lateral hypothalamus in basal conditions and in neuroinflammation [24].

Song and Dityatev investigated the interaction between glia, extracellular matrix and neurons [25]. Lazarevich et al. demonstrated the existence of activity-dependent switches between dynamic regimes of extracellular matrix expression [26]. Rozhnova et al. showed the impact of the brain extracellular matrix on neuronal firing reliability and spike-timing jitter [27]. Rozhnova demonstrated the chaotic change of extracellular matrix molecules concentration in the presence of periodically varying neuronal firing rate [28]. Rozhnova et al. performed bifurcation analysis calculations on a model of brain extracellular matrix [29].

This work aims to perform bifurcation and multiobjective nonlinear model predictive control(MN-LMPC) on two brain dynamics models, which are Brain extracellular matrix model of Rozhnova et al. and the Hodgkin-Huxley model of Xie et al. [29,10]. This document is organized as follows. The model equations for both the models are first described. This is followed by a description of the numerical methods (bifurcation analysis and MNLMPC). The results and discussion are then presented, followed by the conclusions.

Brain Dynamics models Model 1 : Brain extracellular matrix model Rozhnova et al. [29]

The equations in this model are

$$\frac{dzval}{dt} = -(\alpha_z + \gamma_p)zval + \beta_z F_z$$

$$\frac{dpval}{dt} = -\alpha_p pval + \beta_p F_p$$

$$F_z = Z_0 - \frac{Z_0 - Z_1}{1 + \exp(\frac{-Q - \theta_z}{k_z})}$$

$$F_p = Z_0 - \frac{P_0 - P_1}{1 + \exp(\frac{-Q - \theta_p}{k_p})}$$

$$Q = Q_0 + \alpha_Q zval$$
(1)

The parameter values are

$$\begin{split} Q_0 &= 5; \alpha_{\mathcal{Q}} = 0.23; \alpha_{\mathcal{Z}} = 0.001; \alpha_{\mathcal{P}} = 0.001; \gamma_{\mathcal{P}} = 0.001; \beta_{\mathcal{Z}} = 0.01; \\ z_0 &= 0; z_1 = 1; p_0 = 0; p_1 = 1; k_z = 0.15; k_p = 0.05; \beta_p = 0.01 \end{split}$$

zval and pval represent the concentration of the ECM molecules and the concentration of proteases. θ_z, θ_p are the activation midpoints and are the bifurcation and control parameters.

Model 2: Hodgkin-Huxley model (Xie et al. (2008)[10])

The equations in this model are

$$\frac{d(wal)}{dt} = \frac{1}{C_M} (I_{EXT} - g_{Na}(mval)^3 hval(vval - vna) - g_K(mval)^4 (wal - v_K) - g_L(vval - v_L))$$

$$\frac{d(mval)}{dt} = \alpha_m (1 - mval) - \beta_m (mval)$$

$$\frac{d(hval)}{dt} = \alpha_h (1 - hval) - \beta_h (hval)$$

$$\frac{d(mval)}{dt} = \alpha_h (1 - hval) - \beta_h (hval)$$

$$\frac{d(mval)}{dt} = \alpha_n (1 - hval) - \beta_n (hval)$$
(2)

Where $\alpha_{\!\!{}_m},\beta_{\!\!{}_m},\alpha_{\!\!{}_h},\beta_{\!\!{}_h},\alpha_{\!\!{}_n},\beta_{\!\!{}_n}$ are defined as

$$\alpha_{m} = 0.1 \frac{(25 - vval)}{\{\exp(\frac{25 - vval}{10}) - 1\}}$$

$$\beta_{m} = 4 \exp(-\frac{vval}{18})$$

$$\alpha_{h} = 0.07 \exp(-\frac{vval}{20})$$

$$\beta_{h} = \frac{1}{\{\exp(\frac{30 - vval}{10}) + 1\}}$$

$$\alpha_{n} = \frac{0.01(10 - vval)}{\{\exp(\frac{10 - vval}{10}) - 1\}}$$

$$\beta_{n} = 0.125 \exp(-\frac{vval}{80})$$

The parameters are

$$V_{Na} = 115.0 \; , V_{K} = -12.0 \; , \; V_{L} = 10.599, g_{Na} = 120.0, g_{K} = 36 \; , g_{L} = 0.3, C_{M} = 120.0, g_{K} = 12$$

vval is the electrical potential difference voltage across the nerve membrane (membrane potential). mval and hval represent the gating variables for the activation and inactivation of the sodium ion channel, respectively.

nval is the activation gating variable of the potassium ion channel. $I_{\rm EXT}$ is the external current and the bifurcation and control parameter.

Numerical Procedures Bifurcation Analysis

The MATLAB software MATCONT is used to perform the bifurcation calculations. Bifurcation analysis deals with multiple steady-states and limit cycles. Multiple steady states occur because of the existence of branch and limit points. Hopf bifurcation points cause limit cycles . A commonly used MATLAB program that locates limit points, branch points, and Hopf bifurcation points is MATCONT [30,31]. This program detects Limit points (LP), branch points (BP), and Hopf bifurcation points(H) for an ODE system

$$\frac{dx}{dt} = f(x, \alpha) \tag{3}$$

 $x \in \mathbb{R}^n$ Let the bifurcation parameter be a Since the gradient is orthogonal to the tangent vector,

The tangent plane at any point

$$w = [w_1, w_2, w_3, w_4, ..., w_{n+1}]$$
 must satisfy $Aw = 0$ (4)

Where A is

$$A = [\partial f / \partial x | \partial f / \partial \alpha]$$
 (5)

where $\partial f / \partial x$ is the Jacobian matrix. For both limit and branch points, the matrix $[\partial f / \partial x]$ must be singular. The n+1 th component of the tangent vec-

tor $W_{n+1} = 0$ for a limit point (LP)and for a branch

point (BP) the matrix $\begin{bmatrix} A \\ w^T \end{bmatrix}$ must be singular. At a Hopf bifurcation point,

$$\det(2f_x(x,\alpha)@I_n) = 0$$
(6)

@ indicates the bialternate product while I_n is the n-square identity matrix. Hopf bifurcations cause limit cycles and should be eliminated because limit cycles make optimization and control tasks very difficult. More details can be found in Kuznetsov and Govaerts [32-34].

Hopf bifurcations cause unwanted oscillatory behavior and limit cycles. The tanh activation function

(where a control value u is replaced by) ($u \tanh u / \varepsilon$) is commonly used in neural nets and optimal control problems to eliminate spikes in the optimal control profile. Hopf bifurcation points cause oscillatory behavior [35-38]. Oscillations are similar to spikes, and the results in demonstrate that the tanh factor also eliminates the Hopf bifurcation by preventing the occurrence of oscillations [39]. Sridhar explained with several examples how the activation factor involving the tanh function successfully eliminates the limit cycle causing Hopf bifurcation points [39]. This was because the tanh function increases the time period of the oscillatory behavior, which occurs in the form of a limit cycle caused by Hopf bifurcations.

Multiobjective Nonlinear Model Predictive Control (MNLMPC)

Flores Tlacuahuaz et al. developed a multiobjective nonlinear model predictive control (MNLMPC) method that is rigorous and does not involve weighting functions or additional constraints [40]. This procedure is used for performing the MNLMPC calculations

Here $\sum_{t_{i=0}}^{t_i=t_f} q_j(t_i)$ (j=12...n) represents the variables that

need to be minimized/maximized simultaneously for a problem involving a set of ODE

$$\frac{dx}{dt} = F(x, u) \tag{7}$$

t_f being the final time value, and n the total number of objective variables and . u the control parameter. This MNLMPC procedure first solves the single objective optimal control problem independently optimizing

each of the variables $\sum_{t_{i=0}}^{t_i=t_f} q_j(t_i)$ individually. The

minimization/maximization of $\sum_{t_{i=0}}^{t_i=t_f} q_j(t_i)$

will lead to the values q_j^* Then the optimization problem that will be solved is

$$\min\left(\sum_{j=1}^{n} \left(\sum_{t_{i=0}}^{t_i=t_f} q_j(t_i) - q_j^*\right)\right)^2$$

$$subject \ to \ \frac{dx}{dt} = F(x, u); \tag{8}$$

This will provide the values of u at various times. The first obtained control value of u is implemented and the rest are discarded. This procedure is repeated until the implemented and the first obtained control values are the same or if the Utopia point where

$$(\sum_{t_{i=0}}^{t_i=t_f} q_j(t_i) = q_j^* \text{ for all j})$$
 is obtained. Pyomo is used

for these calculations. Here, the differential equations are converted to a Nonlinear Program (NLP) using the orthogonal collocation method The NLP is solved using IPOPT and confirmed as a global solution with BARON [41-43].

The steps of the algorithm are as follows

- 1. Optimize $\sum_{t_{i=0}}^{t_i=t_f} q_j(t_i)$ and obtain q_j^* at various time intervals ti. The subscript i is the index for each time step.
- 2. Minimize $(\sum_{j=1}^{n} (\sum_{t_{i}=0}^{t_{i}=t_{f}} q_{j}(t_{i}) q_{j}^{*}))^{2}$ and get the control values for various times.
- 3. Implement the first obtained control values
- 4. Repeat steps 1 to 3 until there is an insignificant difference between the implemented and the first obtained value of the control variables or if the Utopia point is achieved. The Utopia point is

when
$$\sum_{t_{i=0}}^{t_i=t_f} q_j(t_i) = q_j^*$$
 for all j.

Results and Discussion

For the bifurcation analysis in model 1, θ_p both and θ_p were individually used as bifurcation parameters. When θ_p was used as a bifurcation parameter, two Hopf bifurcation points were found at $(zval, pval, \theta_p)$ values of ($2.128943 \ 0.426793 \ 5.645178$) and ($4.230053 \ 1.696697 \ 6.052311$). These Hopf bifurcation points are shown in Figure 1a

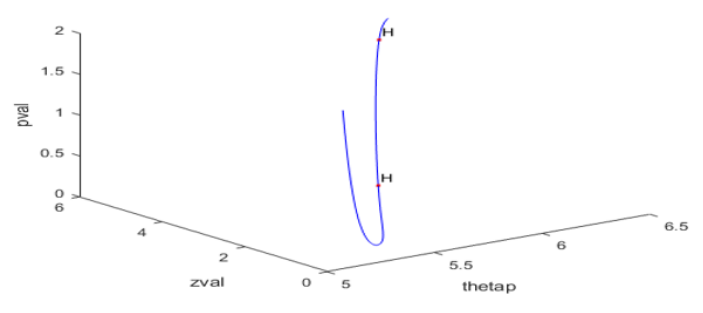


Figure 1a

Each of these Hopf bifurcation points result in a limit cycle which are shown in figures 1b and 1c.

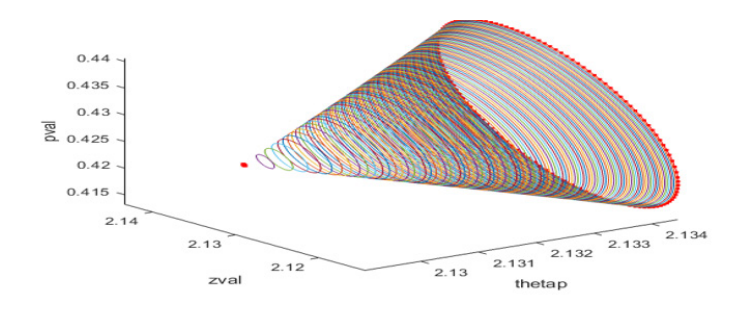


Figure 1b

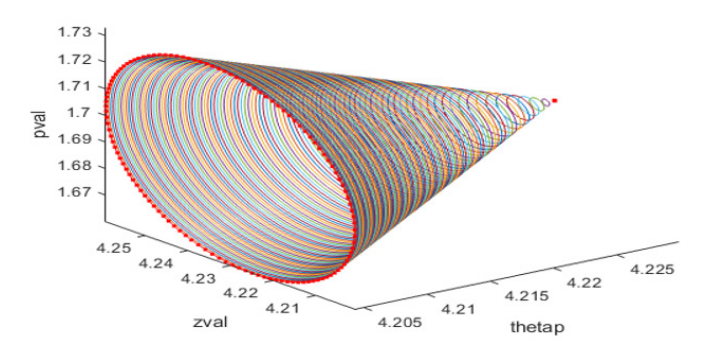


Figure 1c

When θ_p was modified to $\frac{\theta_p \tanh(\theta_p)}{1.115}$ the hopf bifurcations disappear (Figure 1d).

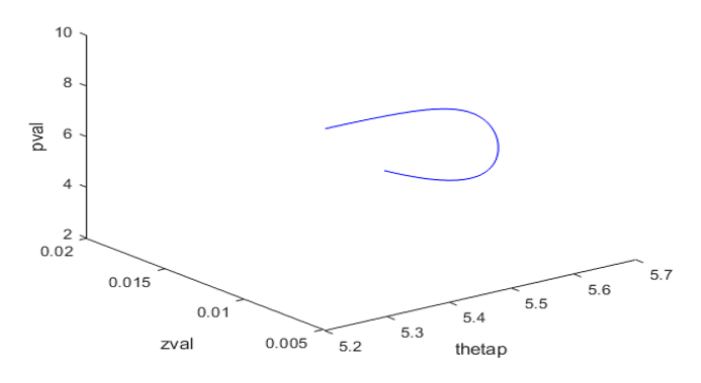


Figure 1d

When θ_2 was used as a bifurcation parameter, two Hopf bifurcation points were found at $(x \cdot d, p \cdot al, \theta_2)$ values of (2.696435 0.266904 5.951550) and (3.190589 2.102711 5.604739) These Hopf bifurcation points are shown in Figure 1e.



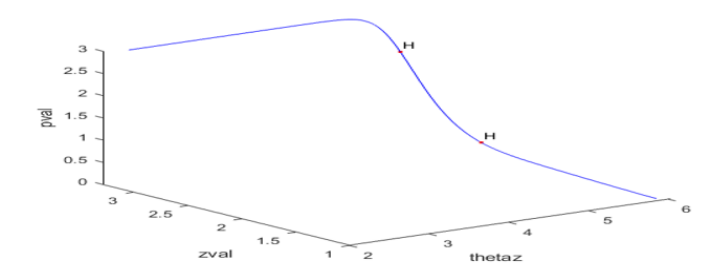


Figure 1e

Each of these Hopf bifurcation points result in a limit cycle which are shown in figures 1f and 1g.

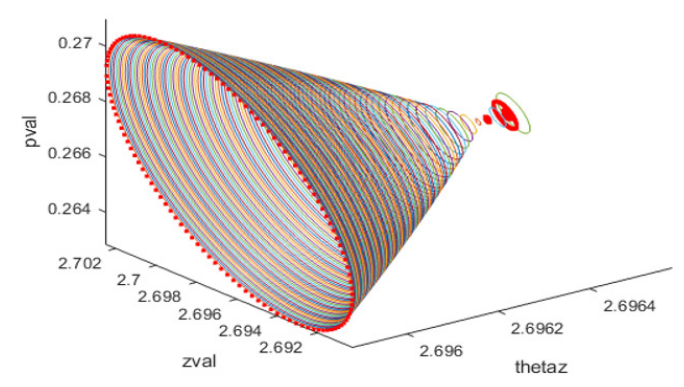


Figure 1f

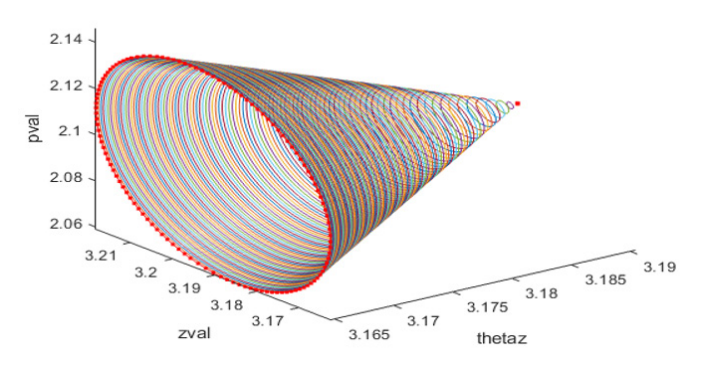


Figure 1g

When θ_z was modified to $\frac{\theta_z \tanh(\theta_z)}{1.115}$ the hopf bifurcations disappear (Figure 1h).

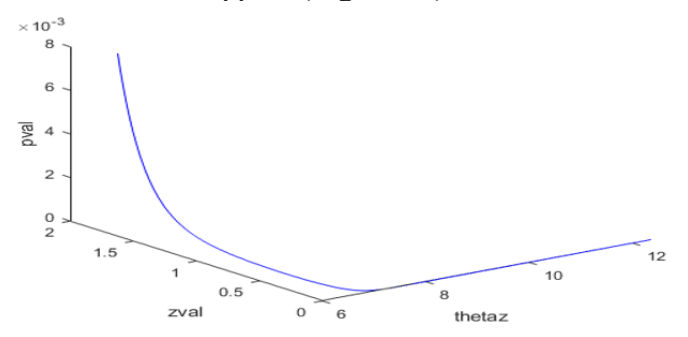


Figure 1h

The MNLMPC calculations were performed using $\frac{\theta_p \tanh(\theta_p)}{1.115}$ and $\frac{\theta_z \tanh(\theta_z)}{1.115}$ as the control

parameters. $\sum_{t_{i=0}}^{t_i=t_j} zval_j(t_i)$ (ECM concentration) was

maximized and resulted in a value of 20. $\sum_{t_{i=0}}^{t_i=t_j} pval_j(t_i)$

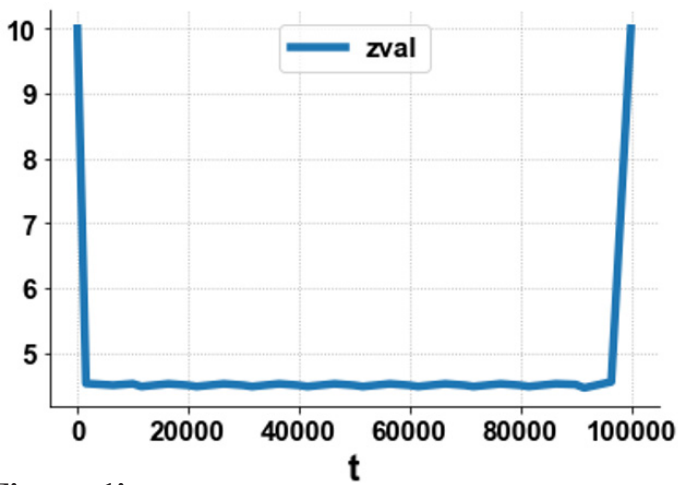
(proteas concentration) was minimized and

resulted in a value of 0. The multiobjective optimal

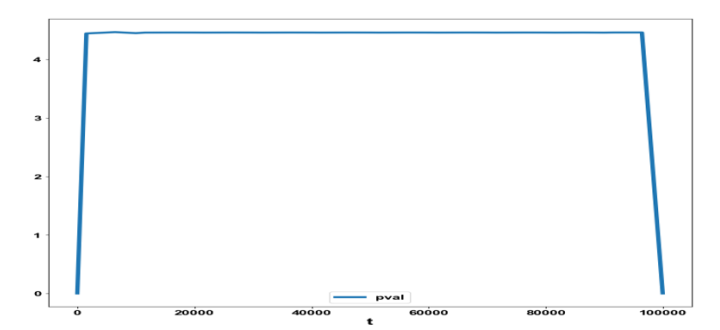
control calculation involved a minimization of

$$(\sum_{t_{i=0}}^{t_i=t_f} zval_j(t_i) - 20)^2 + (\sum_{t_{i=0}}^{t_i=t_f} pval_j(t_i) - 0)^2$$

minimization resulted in the Utopia point (0). The first of the control variables is implemented, and the rest are discarded. The process is repeated until the difference between the first and second values of the control variables are the same. The MNLMPC control values of both θ_p and θ_z were 5 and 5. The zval and pval profiles are shown in Figures 1i and 1j.



Figures 1i



Figures 1j

In model 2, $I_{\rm EMT}$ is the bifurcation parameter and a Hopf bifurcation point was found at (vval, mval, hval, nval, 2, $I_{\rm EMT}$) values of (5.345857 0.097257 0.406228 0.401784 9.779639). This is shown in Figure 2a.

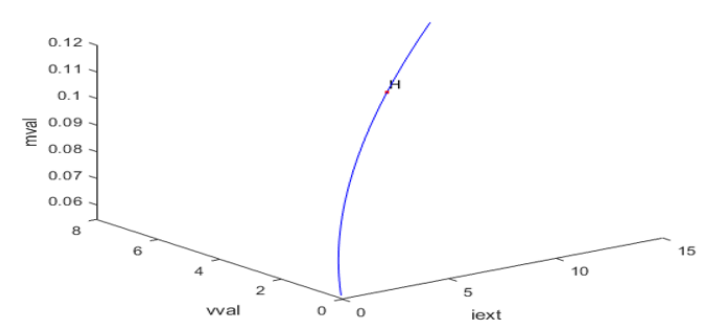


Figure 2a.

The limit cycle produced by this Hopf bifurcation is shown in Figure 2b.

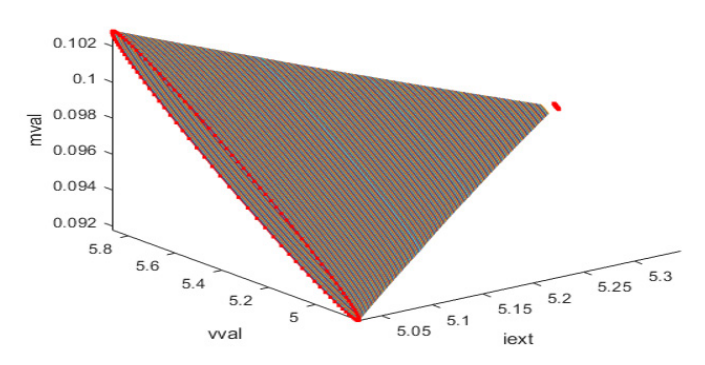


Figure 2b

When I_{EXT} is modified to $\frac{I_{\text{EXT}} \tanh(I_{\text{EXT}})}{1.5}$ the Hopt Bifurcation point disappears.

For the MNLMPC calculations,

$$\sum_{t_{i=0}}^{t_{i}=t_{f}} vval_{j}(t_{i}), \sum_{t_{i=0}}^{t_{i}=t_{f}} mval_{j}(t_{i}), \sum_{t_{i=0}}^{t_{i}=t_{f}} nval_{j}(t_{i})$$

were maximized and resulted in values of 20,20 and

17.3647.
$$\sum_{t_i=t_j}^{t_i=t_j} hval_j(t_i),$$

was minimized and resulted in a value of 0.

The multiobjective optimal control calculation involved a minimization of

$$\left(\sum_{t_{i=0}}^{t_i=t_f} vval_j(t_i) - 20\right)^2 + \left(\sum_{t_{i=0}}^{t_i=t_f} mval_j(t_i) - 20\right)^2$$

$$\left(\sum_{t_{i=0}}^{t_i=t_f} nval_j(t_i) - 17.3647\right)^2 + \left(\sum_{t_{i=0}}^{t_i=t_f} hval_j(t_i) - 0\right)^2$$

was used as the control parameter.

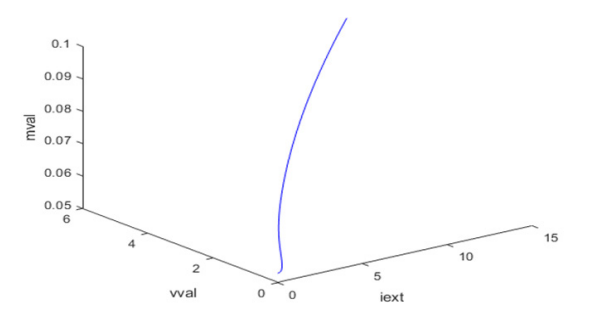


Figure 2c

This minimization resulted in the Utopia point (0). The first of the control variables is implemented, and the rest are discarded. The process is repeated until the difference between the first and second values of the control variables are the same. The MNLMPC control value of is 1. The vval, hval and nval profiles for the MNLMPC calculations are shown in figures 2d and 2e. The mval value was 1 throughout.

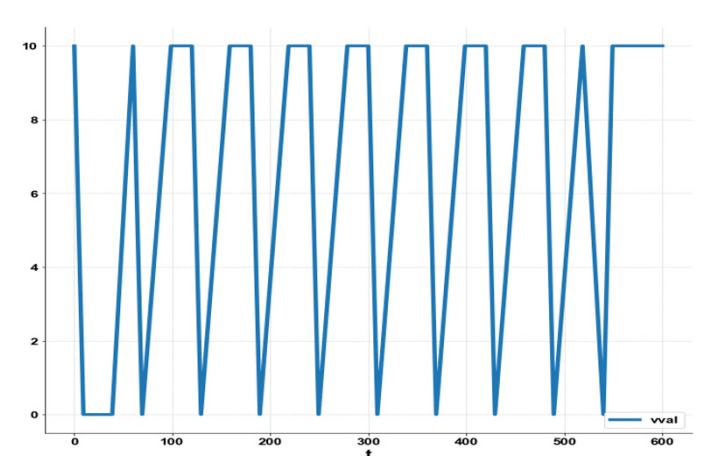


Figure 2d

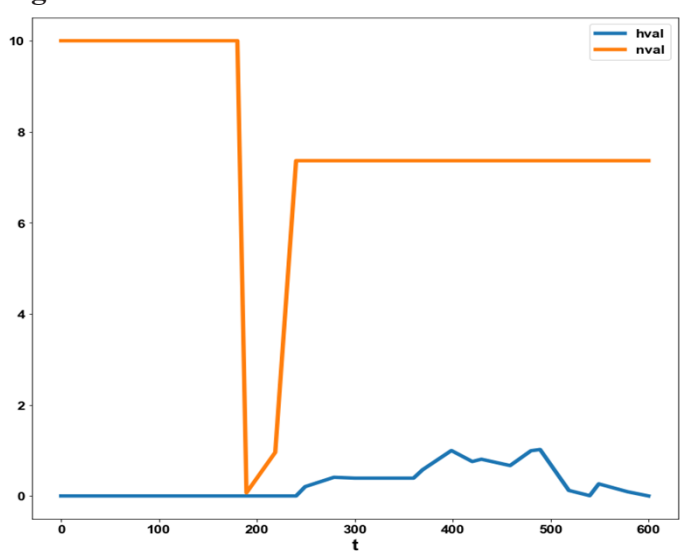


Figure 2e

Both brain models show the presence of limit cycles causing Hopf bifurcations, which can be eliminated using the activation factor involving the tanh function, confirming the analysis of Sridhar(2024). In both cases, the MNLMPC calculations converge to the Utopia solution.

Conclusions

Multiobjective nonlinear model predictive control calculations were performed along with bifurcation analysis on two models involving brain dynamics. The bifurcation analysis revealed the existence of limit cycle causing Hopf bifurcation points, which are eliminated using an activation factor involving the tanh function. The multiojective nonlinear model predictive calculations converge to the Utopia point(the best possible solution) .in both models.

Data Availability Statement

All data used is presented in the paper

Conflict of Interest

The author, Dr. Lakshmi N Sridhar has no conflict of interest.

Acknowledgement

Dr. Sridhar thanks Dr. Carlos Ramirez and Dr. Suleiman for encouraging him to write single-author papers.

References

- 1. Yamaguchi Y (2000) Lecticans: organizers of the brain extracellular matrix. Cellular and Molecular Life Sciences: CMLS 57: 276-289.
- 2. Manor Y, Nadim F (2001) Synaptic depression mediates bistability in neuronal net- works with recurrent inhibitory connectivity. J Neurosci 21: 9460-9470.
- 3. Oohashi T, Hirakawa S, Bekku Y, Rauch U, Zimmermann DR, et al. (2002) Brall, a brain-specific link protein, colocal- izing with the versican v2 isoform at the nodes of ranvier in developing and adult mouse central nervous systems. Mol. Cell. Neurosci 19: 43-57.
- 4. Bekku Y, Su W-D, Hirakawa S, Fässler R, Ohtsuka A, et al. (2003) Molecular cloning of bral2, a novel brain-specific link protein, and immunohistochemical colocalization with brevican in perineuronal nets. Mol. Cell. Neurosci.

24: 148-159

- 5. Dityatev A, Schachner M (2003) Extracellular matrix molecules and synaptic plastic- ity. Nat Rev Neurosci 4: 456-468.
- 6. Carulli D, Rhodes KE, Brown DJ, Bonnert TP, Pollack SJ, et al. (2006) Composition of perineuronal nets in the adult rat cerebellum and the cellular origin of their components. J Comp Neurol 494: 559-577.
- 7. Rich MM, Wenner P (2007) Sensing and expressing homeostatic synaptic plasticity. Trends Neurosci 30:119-125.
- 8. Dityatev A, Brückner G, Dityateva G, Grosche J, Kleene R, et al. (2007) Activi- ty-dependent formation and functions of chondroitin sulfaterich extracellular matrix of perineuronal nets. Dev Neurobiol 67: 570-588.
- 9. Turrigiano G (2007) Homeostatic signaling: the positive side of negative feedback. Curr Opin Neurobiol 17: 318-324.
- 10. Xie, Yong Chen, Luonan Kang, Yan Mei, Aihara (2008) Kazuyuki Controlling the onset of Hopf bifurcation in the Hodgkin-Huxley model, Phys. Rev. E 77.
- 11. Cingolani LA, Lorenzo A, Thalhammer A, Lily MY, Yu LMY, et al. (2008) Activity-dependent regulation of synaptic AMPA receptor composition and abundance by beta 3 integrins. Neuron 58: 749-762.
- 12. Durstewitz D (2009) Implications of synaptic biophysics for recurrent network dynamics and active memory. Neural Networks 22: 1189-1200.
- 13. Dityatev A (2010) Remodeling of extracellular matrix and epileptogenesis. Epilepsia 5: 61-65.
- 14. Kochlamazashvili G, Henneberger C, Bukalo O, Dvoretskova E, Senkov O, et al. (2010) The extracellular matrix molecule hyaluronic acid regulates hip- pocampal synaptic plasticity by modulating postsynaptic l-type ca(2+) chan- nels. Neuron 67: 116128.
- 15. Dityatev A, Schachner M, Sonderegger P (2010) The dual role of the extra- cellular matrix in synaptic plasticity and homeostasis. Nat Rev Neurosci 11: 735-746.
- 16. Dityatev A, Rusakov D (2011) Molecular signals of plasticity at the tetrapartite synapse. Curr Opin Neurobiol 21: 353-359.
- 17. Wlodarczyk J, Mukhina I, Kaczmarek L, Dityatev A (2011) Extracellular matrix molecules, their

J. of Clin Tri Case Reports

receptors, and secreted proteases in synaptic plasticity. Dev Neurobiol 71: 1040-1053.

- 18. Kazantsev V, Gordleeva S, Stasenko S, Dityatev A (2012) A homeostatic model of neuronal firing governed by feedback signals from the extracellular matrix. PLoS ONE 7: e41646.
- 19. Soleman S, Filippov MA, Dityatev A, Fawcett JW (2013) Targeting the neural extracellular matrix in neurological disorders. Neuroscience 253: 194-213.
- 20. Dembitskaya Y, Song I, Doronin M, Dityatev A, Semyanov A () Effects of enzy- matic removal of chondroitin sulfates on neural excitability and synaptic plasticity in the hippocampal CA1 region. 9th FENS Meeting, Milan, Italy 5-9.
- 21. Favuzzi E, Marques-Smith A, Deogracias R, Winterflood CM, Sánchez-Aguil- era A, et al. (2017) Activity-dependent gating of parvalbumin interneuron function by the perineuronal net protein brevican. Neuron 95: 639-655.
- 22. Jercog D, Roxin A, Barthó P, Luczak A, Compte A, et al. (2017) UP-DOWN Cortical dynamics reflect state transitions in a bistable network. Elife 6: e22425.
- 23. Schmidt H, Avitabile D, MontbrióE, Roxin A (2018) Network mechanisms un-derlying the role of oscillations in cognitive tasks. PLoS Comput Biol 14: e1006430.
- 24. Azeez IA, Tesoriero C, Scambi I, Mariotti R, Bentivoglio M (2018) Diurnal fluctuation of extracellular matrix organization in the lateral hypothalamus in basal conditions and in neuroinflammation. 11th FENS Forum of Neuroscience, Berlin 7-11.
- 25. Song I, Dityatev A (2018) Crosstalk between glia, extracellular matrix and neurons. Brain Res Bull 136: 101-118.
- 26. Lazarevich I, Stasenko S, Rozhnova M, Pankratova E, Dityatev A, et al. (2020) Activity-dependent switches between dynamic regimes of extracellular matrix expression. PLoS ONE 5: e0227917.
- 27. Rozhnova MA, Pankratova EV, Kazantsev VB (2020) Brain extracellular matrix impact on neuronal firing reliability and spike-timing jitter. In: Advances in Neural Computation, Machine Learning, and Cognitive Research III (Part of the Studies in Computational Intelligence book series 856: 190-196.

- 28. Rozhnova MA, Bandenkov DV, Kazantsev VB, Pankratova EV (2021) Chaotic change of extracellular matrix molecules concentration in the presence of periodically varying neuronal firing rate. Communications in Computer and Information Science, Mathematical Modeling and Supercomputer Technologies 1413: 117-128.
- 29. Rozhnova MA, Evgeniya V Pankratova, Sergey V Stasenko, Victor B Kazantsev (2021) Bifurcation analysis of multistability and oscillation emergence in a model of brain extracellular matrix, Chaos, Solitons & Fractals 151: 111253.
- 30. Dhooge A, Govearts W, Kuznetsov AY (2003) MATCONT: "A Matlab package for numerical bifurcation analysis of ODEs", ACM transactions on Mathematical software 29: 141-164.
- 31. Dhooge A, W Govaerts, YA Kuznetsov, W Mestrom (2004) Riet, "CL_MATCONT"; A continuation toolbox in Matlab.
- 32. Kuznetsov YA (1998) Elements of applied bifurcation theory. Springer,NY.
- 33. 33. Kuznetsov YA (2009) Five lectures on numerical bifurcation analysis, Utrecht University, NL.
- 34. Govaerts JF (2000) Numerical Methods for Bifurcations of Dynamical Equilibria, SIAM.
- 35. Dubey SR, Singh SK, Chaudhuri BB (2022) Activation functions in deep learning: A comprehensive survey and benchmark. Neurocomputing 503: 92-108.
- 36. Kamalov AF, Nazir M, Safaraliev AK, Cherukuri, R Zgheib (2021) Comparative analysis of activation functions in neural networks, 2021 28th IEEE International Conference on Electronics, Circuits, and Systems (ICECS), Dubai, United Arab Emirates 1-6.
- 37. Szandała T (2020) Review and Comparison of Commonly Used Activation Functions for Deep Neural Networks. ArXiv https://doi. org/10.1007/978-981-15-5495-7.
- 38. Sridhar LN (2023) Bifurcation Analysis and Optimal Control of the Tu¬mor Macrophage Interactions. Biomed J Sci & Tech Res 53.
- 39. Sridhar LN (2024) Elimination of oscillation causing Hopf bifurcations in engineering problems. Journal of Applied Math 2: 1826.
- 40. Flores-Tlacuahuac A (2012) Pilar Morales and Martin Riveral Toledo; "Multiobjective Nonlinear model predictive control of a class of chemical

Review Article Open Access

- reactors". I & EC research 5891-5899.
- 41. Hart William E, Carl D, Laird Jean-Paul Watson, David L Woodruff, Gabriel A Hackebeil, et al. (2021) Pyomo Optimization Modeling in Python' Second Edition 67.
- 42. Wächter A, Biegler L (2006) On the implementation of an interior-point filter line-
- search algorithm for large-scale nonlinear programming". Math. Program 106: 25-57.
- 43. Tawarmalani M, NV Sahinidis (2005) A polyhedral branch-and-cut approach to global optimization", Mathematical Programming 103: 225-249.

Copyright: ©2025 Lakshmi N Sridhar. This is an open-access article distributed under the terms of the Creative Commons Attribution License, which permits unrestricted use, distribution, and reproduction in any medium, provided the original author and source are credited.